False-Positive Whole-Body Iodine-131 Scan Due to Intrahepatic Duct Dilatation

Dong-Ling You, Kai-Yuan Tzen, Jung-Fu Chen, Pan-Fu Kao and Ming-Fong Tsai
Departments of Nuclear Medicine and Metabolism, Chang Gung Memorial Hospital, Taipei, Taiwan

Focal retention of radioactivity in the liver on whole-body ^{131}I scan was interpreted as a metastatic lesion in a patient with well-differentiated thyroid cancer. Intrahepatic duct dilatation, usually resulting from biliary tract obstruction by bile stone, is a common disorder and may cause bile stasis. A patient with papillary thyroid cancer and a previous history of biliary tract stones had focal retention of radioactivity in the liver on whole-body ^{131}I scan. Abdominal CT, endoscopic retrograde cholagiopancreatography, radionuclide cholangiography and sequential ^{131}I scans demonstrated that this focal retention of radioactivity was caused by intrahepatic duct dilatation. Focal retention of radioactivity is visualized on delayed images but not on early images. The radioactivity initially increases and then decreases on following days.

Key Words: thyroid cancer; iodine-131; biliary tract stasis

J Nucl Med 1997; 38:1977–1979

Although biliary tract stone is a common disorder (*1–5*), eastern Asia has a higher prevalence than any other region (*4,5*). Biliary tract stone may obstruct the bile ducts and result in common bile duct (CBD) or intrahepatic duct (IHD) dilatation with stasis of bile (*6*).

The whole-body ^{131}I scan is a sensitive tool to detect metastatic lesion from well-differentiated thyroid cancer (*7,8*). Many false-positive results, however, have been reported in the literature (*9–12*). Focal retention of radioactivity in liver on whole-body ^{131}I scans is usually interpreted as a metastatic lesion (*13,14*). We present a case with papillary thyroid cancer and previous history of gallbladder and CBD stones having a focal retention of radioactivity in the liver on the whole-body ^{131}I scan. Further evaluation revealed it was caused by IHD dilatation.

CASE REPORT

A 56-yr-old woman with papillary thyroid cancer had already had a subtotal thyroidectomy. She had a previous history of cholecystectomy and choledocholithotomy because of gallbladder and CBD stones 1 yr before the papillary thyroid cancer was diagnosed.

After a subtotal thyroidectomy, the thyroglobulin (Tg) level was <10 ng/ml. A diagnostic whole-body ^{131}I scan performed 3 days after taking 185 MBq (5 mCi) ^{131}I revealed two focal remnants in the neck region. There was no other abnormal focal area of retention of radioactivity in the whole-body survey including the hepatic region.

Following ablation of thyroid remnants with 1110 MBq (30 mCi) ^{131}I, whole-body imaging was performed 10 days later. The whole-body ^{131}I scan revealed the two remnants in the neck region and an abnormal focal area of retention of radioactivity in liver (Fig. 1A). For localization, a liver scan was arranged. The liver scan performed after injection of 222 MBq (6 mCi) ^{99m}Tc-sulfur colloid showed a cold defect at the medial portion of the left lobe of the liver (Fig. 1B) corresponding to the area of focal liver retention of radioactivity on whole-body ^{131}I scan. Because of a focal retention of radioactivity on ^{131}I scan and a cold area on liver scan, liver metastasis was considered initially.

Abdominal CT revealed a left IHD dilatation corresponding to the area of focal liver retention of radioactivity on the whole-body ^{131}I scan; no mass lesion was found in the liver (Fig. 1C). The endoscopic retrograde cholangiopancreatography (ERCP) also revealed dilated CBD and left IHD (Fig. 1D).

For the differential diagnosis of IHD dilatation from liver metastasis, radionuclide cholangiography and sequential ^{131}I scans were arranged. Radionuclide cholangiography performed after injection of 222 MBq (6 mCi) ^{99m}Tc-2,6-diisopropyl iminodiacetic

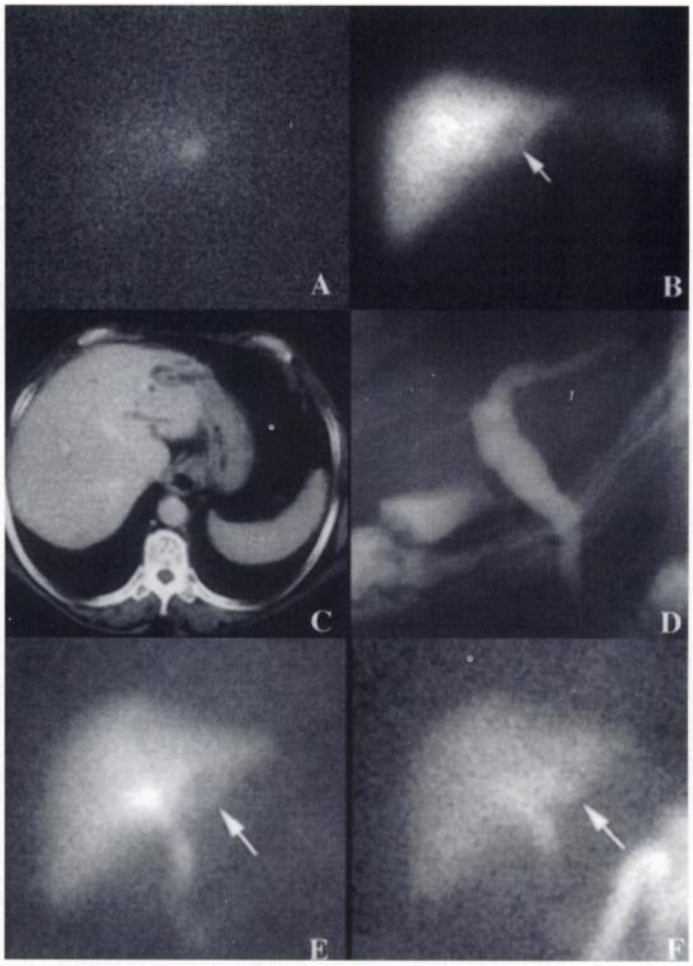

FIGURE 1. Hepatic view of therapeutic whole-body ^{131}I scan (A), liver scan (B), abdominal CT (C), ERCP (D) and radionuclide cholangiography at 5 min (E) and 2 hr (F). There was a focal retention of radioactivity at the left lobe of the liver on whole-body ^{131}I scan corresponding to a cold area seen on liver scan (white arrow). Abdominal CT and ERCP showed prominent left IHD dilatation. Radionuclide cholangiography showed a cold area at the left lobe of the liver at 5 min (white arrow) and then the cold area was filled with radioactivity at 2 hr (white arrow).

Received Jan. 9, 1997; accepted Mar. 6, 1997.
For correspondence or reprints contact: Dong-Ling You, MD, Department of Nuclear Medicine, Chang Gung Memorial Hospital, 199, Tung-Hwa North Rd., Taipei, Taiwan, R.O.C.

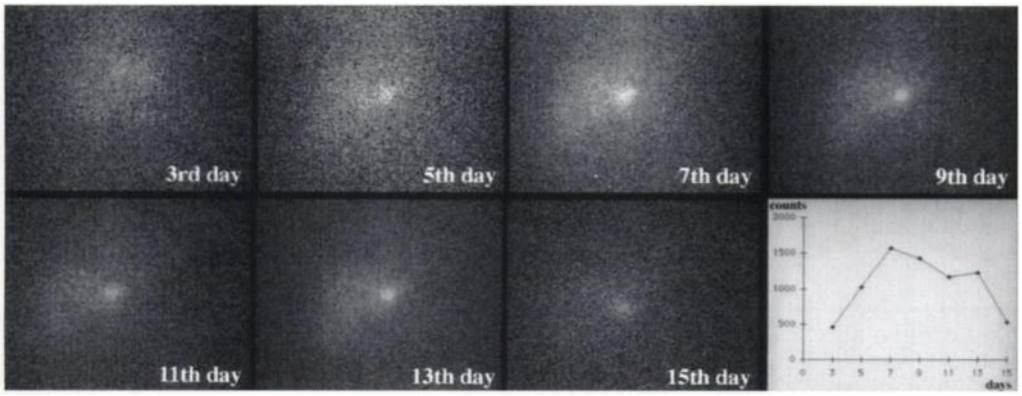

FIGURE 2. Sequential ^{131}I scans and time-activity curve (lower, right). There was no abnormal retention of radioactivity in the liver on the third day. However, a faint retention of radioactivity at the left lobe of the liver was visualized on the fifth day and the radioactivity was increasing by days with the peak activity on the seventh day.

acid revealed a cold area, corresponding to the area of focal liver retention of radioactivity on the whole-body ^{131}I scan, at the medial portion of the left lobe 5 min after injection (Fig. 1E) and then the cold area was filled with radioactivity 2 hr after injection (Fig. 1F). The results suggested the early cold area was dilated IHD.

The sequential ^{131}I scans with hepatic view were performed on the 3rd, 5th, 7th, 9th, 11th, 13th and 15th days after taking 185 MBq (5 mCi) ^{131}I (Fig. 2). The sequential ^{131}I scans revealed no abnormal retention of radioactivity in the liver on the third day. However, a focal area with faint retention of radioactivity at the medial portion of the left lobe of the liver was visualized on the fifth day (Fig. 2). The radioactivity in this focal retention area was increasing and then decreasing gradually by days. The peak radioactivity was visualized on the seventh day. The time-activity curve, using a rectangular region of interest in focal liver retention area and plotted with background subtraction and decay correction, was increasing upward and then decreasing downward by the time of the peak on the seventh day (Fig. 2). The patterns of sequential ^{131}I scans and time-activity curve were similar to that of bile stasis in dilated IHD.

The results of abdominal CT, ERCP, radionuclide cholangiography and sequential ^{131}I scans delineated that the focal retention of radioactivity on the whole-body ^{131}I scan was caused by left IHD dilatation. The patient was well and the Tg levels were <10 ng/ml in a regular 2-yr follow-up at our hospital.

DISCUSSION

Diffuse hepatic visualization on a whole-body ^{131}I scan in cases with well-differentiated thyroid cancer is a normal physiological observation (*15,16*). Focal radioactivity in the liver on the whole-body ^{131}I scan, however, corresponding to a cold area seen on the liver scan is generally a liver metastasis (*13,14*). This case had typical focal retention of radioactivity in the liver corresponding to a cold area on the liver scan. The discrepancy of focal liver retention visualized only on delayed images and not on early images caused consideration of other possibilities such as IHD dilatation.

Well-differentiated thyroid cancer and its metastatic lesion retain the ability to concentrate ^{131}I (*17*). The peak time of ^{131}I uptake by thyroid tissue is between 24 hr and 48 hr (*18*). If liver metastasis occurs, focal retention in the metastatic lesion will be visualized and reaching peak radioactivity within 48 hr (*13,14*). In our case, focal retention of radioactivity in the liver was not visualized on the third day after taking ^{131}I, and that was not like the uptake pattern of metastatic lesion.

Radioiodinated thyroxine is metabolized by the liver into radioiodinated metabolites, which are excreted through the biliary tract system (*19–21*). If biliary tract dilatation occurs, radioiodinated metabolites may stasis in this dilated area. In this situation, focal retention of radioactivity will be visualized on the whole-body ^{131}I scan. Oral ^{131}I incorporated into radioiodinated metabolites takes more than 48 hr (*20,21*). Focal retention of radioactivity is visualized after this period. In this case, the retention of radioactivity was visualized on the fifth day and reached peak radioactivity on the seventh day after taking ^{131}I, suggesting that the focal retention of radioactivity was caused by IHD dilatation and not by liver metastasis.

The pattern of sequential ^{131}I scans and time-activity curve (Fig. 2) are similar as that of bile stasis in dilated IHD. The gradually increasing retention of radioactivity is probably due to production of radioiodinated metabolites faster than bile excretion from dilated IHD. The decreasing retention of radioactivity is probably due to excretion of radioiodinated metabolites from dilated IHD after the production of radioiodinated metabolites has been decreased.

CONCLUSION

Although a focal retention of radioactivity in the liver on the whole-body ^{131}I scan suggests a metastatic lesion, IHD dilatation also may cause such focal retention of radioactivity in the liver. Our article suggests that a focal retention of radioactivity in the liver on the whole-body ^{131}I scan visualized only on delayed scan, but not on early scan, may be caused by IHD dilatation especially in patients having a previous history of biliary tract disease.

REFERENCES

1. Ingelfinger FJ. Digestive disease as a national problem: V. *Gall Gastroenterol* 1968;55:102–104.
2. Almy TP. Prevalence and significance of digestive disease. *Gastroenterology* 1975; 68:1351–1371.
3. Jensen KH, Jorgebsen T. Incidence of gallstones in a Danish population. *Gastroenterology* 1991;100:790–794.
4. Nakayama F, Soloway RD, Nakama T, et al. Hepatolithiasis in East Asia-retrospective study. *Dig Dis Sci* 1986;31:21–26.
5. Su CH, Lui WY, Peng FK. Relative prevalence of gallstone diseases in Taiwan: a nationwide cooperative study. *Dig Dis Sci* 1992;37:764–768.
6. Lu SCL, Kaplowitz N. Diseases of the biliary tree. In: Yamada T, eds. *Textbook of gastroenterology*, 2nd ed. Philadelphia: J.B. Lippincott; 1995:2215–2216.
7. Maxon HR III, Smith HD. Radioiodine in the diagnosis and treatment of metastatic well-differentiated thyroid cancer. *Endocrinol Metab Clin North Am* 1990;19:685–718.
8. Samaan NA, Schultz PN, Hickey RC, et al. The results of various modalities of treatment of well-differentiated thyroid carcinoma: a retrospective review of 1599 patients. *J Clin Endocrinol Metab* 1992;75:714–720.
9. Ceccarelli C, Pacini F, Lippi F, Pinchera A. An unusual case of a false positive iodine-131 whole body scan in a patient with papillary thyroid cancer. *Clin Nucl Med* 1984;9:192–193.
10. Kolla IS, Alazraki NP, Watts N. Sialandinitis mimicking metastatic thyroid cancer. *Clin Nucl Med* 1989;14:564–566.
11. Wu SY, Brown T, Milne N, et al. Iodine 131 total body scan-extrathyroidal uptake of radioiodine. *Semin Nucl Med* 1986;XVI:82–84.
12. Brucker-Davis F, Reynolds JC, Skarulis MC, et al. False-positive iodine-131 whole-body scans due to cholecystitis and sebaceous cyst. *J Nucl Med* 1996;37: 1690–1693.
13. Woolfenden JM, Waxman AD, Wolfstein RS, et al. Scintigraphy evaluation of liver metastasis from thyroid cancer. *J Nucl Med* 1975;16:669–671.
14. Atmaran SH, Ganatra RD, Sharma SM, et al. Functioning metastasis in liver from thyroid cancer. *J Nucl Med* 1975;16:919–921.

15. Ziessman HA, Bahar H, Fahey FH, Dubiansky V. Hepatic visualization on iodine-131 whole-body thyroid cancer scans. *J Nucl Med* 1987;28:1408–411.
16. Rosenbaum RC, Johnston GS, Valente WA. Frequency of hepatic visualization during I-131 imaging for metastatic thyroid carcinoma. *Clin Nucl Med* 1988;13:657–661.
17. Sisson JC. Treatment of thyroid cancer. In: Wagner HN, eds. *Principles of nuclear medicine*, 2nd ed. Baltimore: W.B. Saunders; 1995:629.
18. Cavalieri RR. In vivo isotopic tests and imaging. In: Braverman LE, Utiger RD, eds. *The thyroid: a fundamental and clinical text*. 6th ed. Philadelphia: J.B. Lippincott; 1991:438.
19. Oppenheimer JH. Thyroid hormone in liver. *Mayo Clin Proc* 1972;47:854–863.
20. Griffin JE. The thyroid. In: Griffin JE, Oieda SR, eds. *Textbook of endocrine physiology*, 3rd ed. New York: Oxford University Press Inc; 1996:260–265.
21. Engler D, Burger AG. The deiodination of the iodothyronines and of their derevatives in man. *Endo Rev* 1984;5:151–184.

False-Positive Somatostatin Receptor Scintigraphy Due to an Accessory Spleen

R. Lebtahi, G. Cadiot, J.P. Marmuse, C. Vissuzaine, Y. Petegnief, A. Courillon-Mallet, D. Cattan, M. Mignon and D. Le Guludec

Nuclear Medicine, Surgery and Gastroenterology Departments, Bichat Hospital; and Gastroenterology Department, Villeneuve Saint Georges Hospital, Paris, France

A patient with previous left caudal pancreatectomy and splenectomy presented with Zollinger-Ellison syndrome. Abdominal CT and endoscopic ultrasonography revealed a mass in the splenic area. Somatostatin receptor scintigraphy showed a nodular increase of the uptake corresponding to the lesion detected with conventional imaging. A second laparotomy was performed and the mass was resected. Histological analysis showed that the nodular lesion was an accessory spleen. Since physiologic uptake of ^{111}In-pentetreotide is seen in the spleen, an accessory spleen mimicking a tumor, specially after previous splenectomy, may result in false-positive somatostatin receptor scintigraphy.

Key Words: somatostatin receptor scintigraphy; gastroenteropancreatic tumors; accessory spleen

J Nucl Med 1997; 38:1979–1981

Somatostatin receptor scintigraphy (SRS) detects neuroendocrine gastroenteropancreatic (GEP) tumors with a high sensitivity (70% to 95%) (*1–9*). It may detect primary and metastatic endocrine tumors not visualized by other imaging techniques and, therefore, is considered to have an effect on patient's management (*7,8*). Specificity, reported by autoradiographic and clinical studies, seems high but is difficult to evaluate because all scintigraphic positive sites cannot be histologically studied. In our experience of more than 200 patients with neuroendocrine GEP tumors, we report here a case of demonstrated false-positive result due to an accessory spleen.

CASE REPORT

A 63-yr-old man was admitted in July 1988, with epigastric pain, vomiting and diarrhea of a few months duration. The esophagogastroduodenoscopy showed ulcerative esophagitis and ulcerative duodenitis. A diagnosis of Zollinger-Ellison syndrome (ZES) was biologically confirmed on secretin test results: basal acid output 11.7 mmol/hr acid output, after secretin infusion (3 U/kg/hr), 27.7 mmol/hr above our 100% specificity threshold for the diagnosis of ZES; basal gastrin levels 77 microU/ml (normal value < 115); and gastrin under secretin infusion 222 microU/ml (*8*). Abdominal CT scan and ultrasonography were negative, as well as the search for multiple endocrine neoplasia Type 1. In November 1988, an explorative laparotomy was performed. A complete surgical exploration of the abdomen performed without preoperative endoscopy was negative. Intraoperative ultrasonography of the caudal pancreas gave doubtful results. A left caudal pancreatectomy with splenectomy was performed. Histological examination of the resected pancreas was normal. No pathological lymph node was found. No neuroendocrine tumor was found on the resected tissue. The patient was discharged on Omeprazole therapy (60 mg/d).

In May 1994, the secretin test remained positive: basil acid output at 2.3 mmol/hr, acid output under secretin infusion (3U/kg/hr) at 18.6 mmol/hr, basal gastrin levels at 143pg/ml (N < 108), gastrin under secretin infusion at 227pg/ml, confirming the diagnosis of ZES.

Abdominal CT and endoscopic ultrasonography revealed a mass in the splenic area (2.4 cm) near the left kidney, suggesting a tumoral lymph node.

Somatostatin receptor scintigraphy was performed with injection of 135 MBq ^{111}In-pentetreotide. Scintigraphic images were acquired using a dual-head camera (DST Sopha Medical Vision, Brie, France) with a medium-resolution, parallel-hole collimator, and a 256 × 256 word matrix with a preset time of 10 min. Acquisition was adjusted to both ^{111}In photopeaks (171 and 245 keV). Abdominal images were obtained at 4 hr in the anterior and posterior views. At 24 hr, the acquisition included anterior and posterior views for the head, chest and pelvis, and anterior, posterior, lateral and oblique views for the abdomen. Abdominal single emission CT (SPECT) was performed at 24 hr postinjection, using a double indium peak acquisition, 64 projections over 360° rotation, 60 sec per step, 64 × 64 matrix. Slices were reconstructed after backprojection using a Hann filter. Delayed images were performed on the abdomen in the anterior, posterior and lateral views 30 hr postinjection. SRS showed physiological uptake in liver and kidneys; the spleen had been removed previously. A focal increase of tracer uptake was clearly visualized in the left lateral and left posterior oblique views in the splenic area (Fig. 1), corresponding to the lesion detected with CT scan and endoscopic ultrasonography. No other abnormal tumoral uptake was found. A second laparotomy was performed in June 1996, 48 hr after injection of ^{111}In-pentetreotide.

After careful surgical examination of the abdomen, the surgeon found the nodular lesion corresponding to the lesion identified on preoperative imaging (CT, endoscopic ultrasonography and SRS). Intraoperative ultrasonography of the liver, duodenum and pancreas were negative. Intraoperative endoscopy with duodenal transillumination were also negative. Intraoperative scintillation detection performed was negative in the liver, pancreas and

Received Mar. 11, 1997; accepted March 16, 1997.
For correspondence or reprints contact: Rachida Lebtahi, MD, Service de Médecine Nucléaire, Hôpital Bichat, 46 rue Henri Huchard, 75018, Paris, France.